Int J Clin Exp Pathol 2015;8(12):15684-15695
www.ijcep.com /ISSN:1936-2625/IJCEP0017510

Original Article

Curcumin improves bone microarchitecture in glucocorticoid-induced secondary osteoporosis mice through the activation of microRNA-365 via regulating MMP-9

Guowei Li[1*], Juyuan Bu[2*], Yingxian Zhu[3], Xiaoyu Xiao[3], Zibin Liang[4], Rongkai Zhang[1]

Departments of [1]Orthopaedics II, [2]General Surgery I, [3]Anesthesiology, [4]Oral and Maxillofacial Surgery, Fifth Affiliated Hospital of Sun Yat-sen University, Zhuhai 519000, China. [*]Equal contributors.

Received October 9, 2015; Accepted November 20, 2015; Epub December 1, 2015; Published December 15, 2015

Abstract: The present study aimed to investigate bone microarchitecture of the proximal tibia in glucocorticoid-induced osteoporosis (GIOP) mice, and the underlying molecular mechanisms of curcumin in DXM-induced osteoporosis were performed. DXM-treated facilitated to induce hypercalciuria in mice, and curcumin-treated showed a decrease in urine calcium. Curcumin reversed DXM-induced bone resorption, including an increase in serum OCN and a decrease in bone resorption markers CTX and TRAP-5b. H&E staining showed the increased disconnections and separation in trabecular bone network as well as the reduction of trabecular thickness throughout the proximal metaphysis of tibia in GIOP group. Importantly, curcumin reversed DXM-induced trabecular deleterious effects and stimulated bone remodeling. The further evidence showed that curcumin supplement significantly decreased the TRAP-positive stained area and inhibited the activity of OPG/RANKL/RANK signaling in the GIOP mice. Moreover, bioinformatics analysis suggested that miR-365 was a regulator of MMP9. The levels of miR-365 were markedly suppressed; however, curcumin treatment could reverse the downregulation of miR-365 in the tibia of GIOP mice. Simultaneously, the results demonstrated that the mRNA and protein expression of MMP-9 were significantly increased in GIOP mice compared with that of the control group. Curcumin treatment could suppress the expression of MMP-9 in the tibia of GIOP mice. The present study demonstrated the protective effects of curcumin against bone deteriorations in the experimentally DIOP mice, and the underlying mechanism was mediated, at least partially, through the activation of microRNA-365 via suppressing MMP9.

Keywords: Osteoporosis, curcumin, dexamethasone, miR-365, MMP9

Introduction

Glucocorticoids (GCs) have been widely used in clinics due to their anti-inflammatory and immunomodulatory effects. However, the therapeutic use for immunosuppression after organ transplantation or for inflammatory diseases of glucocorticoids is always accompanied by decreasing bone formation and increasing bone resorption and fragility [1]. The mechanisms account for GC-induced inhibition of bone formation including the suppression of osteoblast differentiation, maturation and activity and the reduction of lifespan of osteoblast, which have been regarded as an important cause for osteopenia or osteoporosis [2, 3]. Curcumin is the major active ingredient of turmeric (*Curcuma longa*) and is known to possess potent anti-inflammatory [4] and anti-arthritic [5] properties. In fact, the effects of curcumin on bone cells have previously been investigated *in vitro* [6, 7]. In co-cultures of bone marrow stromal cells (BMSC) and whole bone marrow cells (BMC), exposure to curcumin leads to dose-dependent suppression of osteoclastogenesis in the coculture system and reduces the expression of RANKL in IL-1α-stimulated BMSCs [8]. Therefore, curcumin effects on bone microarchitecture *in vivo* warranted further evaluation. Previous studies have unveiled its action mechanisms to protect against ovariectomy-induced bone changes in rat model [9, 10] and decrease

osteoclastogenesis [11]. In APP/PS1 transgenic mice, curcumin treatment leads to constant increases in the trabecular bone mass of the metaphysis [12]. However, the roles of curcumin in glucocorticoid-induced secondary osteoporosis have not been clearly delineated.

MicroRNAs (miRs) are endogenous non-coding RNAs and single-stranded RNA molecules of 18~22 nucleotides in length that serve as important post-transcriptional gene regulators. The key features of miRs control cell proliferation and differentiation of various cell types. MiRs regulate biological processes by binding to the mRNA 3'-untranslated region (UTR) sequences to attenuate protein synthesis. A growing number of studies have demonstrated that the pathogenic change in various tissues has been linked to miRs [13, 14]. Accumulating evidence points to an intimate connection between miRNAs and bone homeostasis. In mouse preosteoblastic MC3T3-E1 cells, miR-29b promotes osteoblast differentiation in by directly downregulating known inhibitors, HDAC4, TGFb3, ACVR2A, CTNNBIP1 and DUSP2, of osteoblast differentiation via binding to target 3'-UTR sequences in their mRNAs [15]. Moreover, miR-2861 and miR-3960 play a positive role in regulating osteoblast differentiation [16, 17]. In osteoclast differentiation, the expression of has-miR-148a increased, overexpression of miR-148a can promote CD14+ PBMCs differentiation into osteoclasts [18]. The expression of avian musculoaponeurotic fibrosarcoma oncogene homolog B (MAFB) a target gene of miR-148a is inhibited at the post-transcriptional level and indirectly promotes the expression of NFATc1 and OSCAR, which can promote osteoclast differentiation [18]. In RAW264.7 cells, miR-7b is decreased in the present of M-CSF and RANK, however, its overexpression attenuates the number of TRAP-positive cells and the formation of multinucleated cells. In contrast, the inhibition of miR-7b enhances osteoclastogenesis, and miR-7b inhibited osteoclastogenesis and cell-cell fusion by directly targeting DC-STAMP that is associated with expression of NFATc1 and c-fos [19]. These results indicate that alterations in the expression levels of miRs associated with bone metabolism can lead to osteoporosis and other bone diseases. However, the underlying signaling mechanisms accounting for miRs in glucocorticoid-induced osteoporosis (GIOP) are still not well characterized.

In the present study, bioinformatics analysis suggested that miR-365 was a regulator of matrix metalloproteinase-9 (MMP-9). There was a possibility that miR-365 might be involved in glucocorticoid-induced secondary osteoporosis and was utilized as a therapeutic target for curcumin in experimentally GIOP mice.

Materials and methods

Animal treatment

Ten-week-old male C57BL/6J mice (Guangzhou University of Traditional Chinese Medicine, Guangzhou, China) were allowed to acclimate to the environment for 1 week. All experimental procedures were carried out in accordance with the guidelines of the Fifth Affiliated Hospital of Sun Yat-sen University on Animal Care. All chemicals and reagents were purchased from Sigma (Oakville, Ontario, Canada), except where noted. The mice were randomly divided into three groups: (1) Vehicle group (n = 10); (2) Mice were injected intramuscularly with 5 mg/kg body weight dexamethasone (DXM) three times a week for 12 weeks (GIOP, n = 10); (3) Mice in the GIOP group received curcumin orally at a dose of 200 mg/kg per day for 12 weeks (crucumin, n = 10).

Chemistries in serum and urine

The concentrations of calcium (Ca) and creatinine (Cre) in serum and urine were measured by standard colorimetric methods using a micro-plate reader (Bio-Tek, USA). The level of urine Ca was corrected by the concentration of urine Cre. Serum levels of tartrate resistant acid phosphatase-5b (TRACP-5b), Osteocalcin (OCN) and C-terminal telopeptide of type I collagen (CTX) were detected using mouse bioactive ELISA assay (Immutopics, Inc., San Clemente, CA, USA) with ELISA reader (MD SpectraMax M5, USA).

Bone histomorphology

The tibias were decalcified in 0.5 M EDTA (pH = 8.0) and then embedded in paraffin by standard histological procedures. Section of 5 μm were cut and stained with hematoxylin & eosin (H&E), and visualized under a microscope (Leica DM 2500, Germany). Tibias were subjected to an assay for TRAP activity according to the manufacturer's protocol (Sigma Alrich, St

Louis, MO, USA). The images were taken with a digital camera attached to the microscope (Leica DM 2500, Germany). The trabecular bone microarchitecture of the proximal metaphysis of the tibia was measured using a microtomography scanner (SkyScan 1076, Kontizh, Belgium) with a slice thickness of 22 μm. Bone morphometric parameters, including bone volume over total volume (BV/TV), trabecula number (Tb. N), trabecula thickness (Tb. Th) and trabecula separation (Tb. Sp) were measured.

Cell culture and osteoclast differentiation

Osteoblast, MC3T3-E1 and RAW 264.7 maintained in α-MEM containing (Invitrogen, USA) supplemented with 10% FBS (Invitrogen, USA) at 37°C in a humidified incubator (Thermo, USA), 5% CO_2, 95% air atmosphere. The medium was replenished every two days. Bone marrow cells were prepared by removing from tibia and exposed to 50 ng/mL M-CSF and 50 ng/mL RANKL for an additional 14 days. Cells were treated with 100 nM DXM for 72 h. MicroRNA groups were transfected with miR-365 for 48 h.

Overexpression of miR-365 and luciferase reporter gene activity assay

For the transfection of cells, lentiviral vectors harboring miR-365 was constructed, and the cells were infected. The 3'UTR of MMP-9 gene containing the predicated target sites for miR-365 was obtained by PCR amplification. The fragment was inserted into the multiple cloning sites in the pMIR-REPORT luciferase microRNA expression reporter vector (Ambion, Austin, USA). HEK-293 cells were co-transfected with 0.1 μg of luciferase reporters containing MMP-9 3'UTR and miR-365 mimics by Lipofectamine 2000 (Invitrogen, Carlsbad, USA). We harvested the cell lysates after 48 h transfection and measured the luciferase activity with a dual luciferase reporter assay kit according to manufacturer's instruction.

Reverse transcription-polymerase chain reaction

The tibias of each animal were crushed under liquid nitrogen conditions and RNA extraction was performed according to the TRIzol manufacturer's protocol (Invitrogen, Carlsbad, CA, USA). Synthesis of cDNAs was performed by reverse transcription reactions with 2 μg of total RNA using moloney murine leukemia virus reverse transcriptase (Invitrogen) with oligo dT (15) primers (Fermentas) as described by the manufacturer. The first strand cDNAs served as the template for the regular polymerase chain reaction (PCR) performed using a DNA Engine (ABI 7300). Glyceraldehyde 3-phosphate dehydrogenase (GAPDH) as an internal control was used to normalize the data to determine the relative expression of the target genes. The reaction conditions were set according to the kit instructions. The PCR primers used in this study were shown as following: miR-365, Forward 5'-GATCTGCAGGGGTTAGCTTG-3' and Reverse 5'-GATCATATGAGAGTGACATC-3'; ALP, Forward 5'-CCAGGGCGTACGGAGGCCATT-3' and Reverse 5'-GACCAAATTACGGCGTAGCCTC-3'; osteocalcin, Forward 5'-TGGGCATGGCAGTACCCGTTCG-3' and Reverse 5'-CGCCGGTAGTCCGGACCCT-3'; TRAP, Forward 5'-AGCATAAGGGTCCAAGTCCAA-3' and Reverse 5'-TACCAAAAGCGGCGTAGTTA-3'; CTSK, Forward 5'-AGGCGGAGGTCGATGCCCCG-3' and Reverse 5'-CACGATGATGTCACCCTCGATGT-3'; OPG, Forward 5'-ACCGTGAGTTGTCCGTAGCATC-3' and Reverse 5'-CGTAAGGGTCCGATACATCTC-3'; RANK, Forward 5'-CCTCGGGGTCTGGGAGTTCG-3' and Reverse 5'-CGTACACCACGATGATGTCACCCT-3'; RANKL, Forward 5'-CGTAGGTAGCCGGGTAGGATC-3' and Reverse 5'-GCGTGGGAGCCTGATGCTCA-3'; MMP-13, Forward 5'-AGGATGGAATGCCGAGTTCGCAGT-3' and Reverse 5'-CGTGCCCGATGGCAAGTCCCGCT-3'; MMP-9, Forward 5'-CGGTGCCGATGTGGCCGTCATTG-3' and Reverse 5'-CGTAGTGCGGTGAAGGGTCCTA-3'; GAPDH, Forward 5'-ACAGGGGAGGTGATAGCATT-3' and Reverse 5'-GACCAAAAGCCTTCATACATCTC-3'.

Western blotting

The tibias were homogenized and extracted in NP-40 buffer, followed by 5-10 min boiling and centrifugation to obtain the supernatant. Samples containing 50 μg of protein were separated on 10% SDS-PAGE gel, transferred to nitrocellulose membranes (Bio-Rad Laboratories, Hercules, CA, USA). The membranes were incubated with the following antibodies, RANKL, CTSK, MMP-13 and MMP-9 (R&D Systems, Minneapolis, MN, USA), at dilutions ranging from 1:500 to 1:2,000. After three washes with TBST, membranes were incubated with secondary immunoglobulins (Igs) conjugated to

Table 1. Physiological and biochemical properties

	Vehicle	DIOP	Curcumin
Body weight (g)	25.5 ± 3.8	34.2 ± 4.5*	26.3 ± 3.7#
Serum Ca (mg/dL)	10.21 ± 0.46	9.89 ± 0.41	10.57 ± 0.55
Urine Ca/Cre (mg/mg)	0.069 ± 0.007	0.126 ± 0.014*	0.073 ± 0.009#
TRACP-5b (pg/mL)	2.48 ± 0.32	3.92 ± 0.44*	2.83 ± 0.37#
OCN (ng/mL)	479 ± 50.8	315 ± 32.4*	506 ± 59.2#
CTX (ng/mL)	37.7 ± 6.8	74.7 ± 8.9*	48.2 ± 9.2#

Values are expressed as mean ± SD, n = 8-10 in each group. *$P < 0.05$, versus vehicle group; #$P < 0.05$, versus GIOP group. Ca, calcium; Cre, creatinine; TRACP-5b, tartrate resistant acid phosphatase-5b; OCN, osteocalcin; CTX, C-terminal telopeptide of type I collagen.

IRDye 800CW Infrared Dye (LI-COR), including donkey anti-goat IgG and donkey anti-mouse IgG at a dilution of 1:10,000-1:20,000. After 1 hour incubation at 37°C, membranes were washed three times with TBST. Blots were visualized by the Odyssey Infrared Imaging System (LI-COR Biotechnology) and normalized to the β-actin signals to correct for unequal loading using the mouse monoclonal anti-β-actin antibody (Bioworld Technology, USA).

Statistical analysis

The data from these experiments were reported as mean ± standard deviation (SD) for each group. All statistical analyses were performed using PRISM version 4.0 (GraphPad). Intergroup differences were analyzed by one-way ANOVA. Differences with *P* value of < 0.05 were considered statistically significant.

Results

Effects of the dietary supplement of curcumin on physiological and biochemical properties

The body weight and calcium levels in serum and urine were measured in the three experimental groups. The body weight increased in GIOP mice before the curcumin supplement was given, however, the body weight was significantly reduced by the curcumin supplement. No effect of curcumin on serum calcium was observed. Moreover, the urinary calcium level, which significantly increased to 2-fold in GIOP mice as compared to control group, was significantly decreased by the curcumin supplement (**Table 1**). These results indicated that glucocorticoid-treated could accelerate calcium outflow, and curcumin could reverse disequilibrium of calcium homeostasis in GIOP mice. Serum concentrations of bone metabolism markers, like TRAP-5b and CTX as a bone resorption marker, OCN as a bone formation marker, were determined. Serum TRAP-5b and CTX levels in DIOP mice significantly increased to about 1.6- and 2.0-fold of the control value, respectively. These activities were markedly reduced to the control level by the curcumin supplement. The activities of OCN in serum with GIOP mice were decreased to about 66% of the control value. The curcumin supplement could reverse the decreased level of OCN in DIOP mice (**Table 1**). From these biochemical data, it was well shown that curcumin exerted protective effects on DXM-induced bone deteriorations in mice.

Effects of the dietary supplement of curcumin on the mRNA levels of ALP, osteocalcin, TRAP and cathepsin K in the tibias

As shown in **Figure 1**, the results showed that the mRNA levels of ALP were significantly increased when compared to that of the control group, these increases were not restored by the curcumin supplement. Moreover, the mRNA levels of osteocalcin in the GIOP group significantly decreased to about 35% of the control level, these decreases were restored by the curcumin supplement. The mRNA levels of TRAP and cathepsin K in the GIOP mice were significantly higher than that of the control group. However, the increased levels were reduced to the control value by the curcumin supplement (**Figure 1**).

Effects of the dietary supplement of curcumin on bone microarchitecture and osteoclastogenesis

The analysis of trabecular bone microarchitecture in proximal metaphysis of tibia was performed by H&E staining (**Figure 2A**). The histology of trabecular bone below growth plate was markedly different in the three experimental groups. H&E staining showed the increased disconnections and separation in trabecular bone network as well as the reduction of trabecular thickness throughout the proximal metaphysis of tibia in GIOP group. This accounted for the disconnections and separation of trabecular in

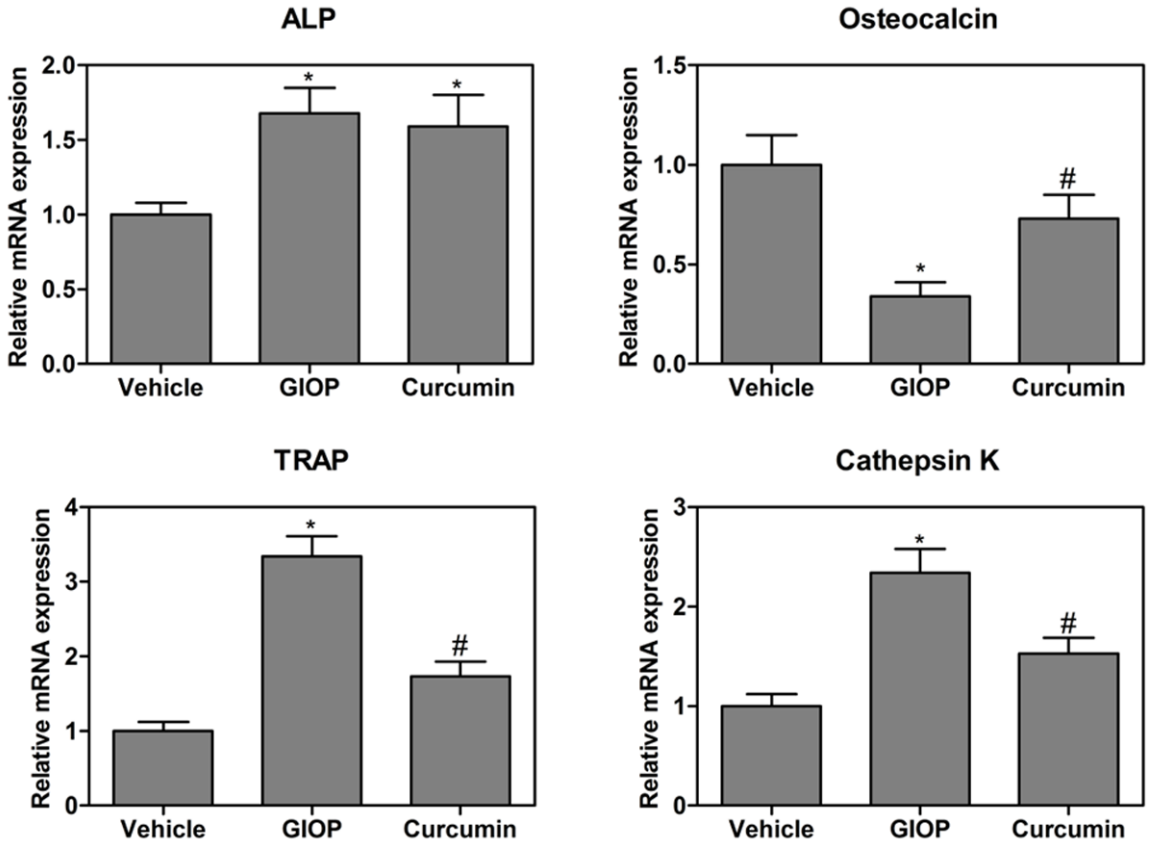

Figure 1. Effects of the dietary supplement of curcumin on the mRNA expression of ALP, osteocalcin, TRAP and cathepsin K in the tibia of mice. Values were expressed as mean ± SD, n = 10 in each group. $^{*}P < 0.05$ versus vehicle group, $^{\#}P < 0.05$ versus GIOP group.

the DIOP group which was due to the process of osteoclastosis resulting in bone resorption. Importantly, curcumin reversed DXM-induced trabecular deleterious effects and stimulated bone remodeling (**Figure 2A**). Importantly, the structural parameters of trabecular bone network in proximal metaphysis of tibia were performed. The results revealed that GIOP mice showed significantly lower trabecular BV/TV, Tb. N, Tb. Th and Tb. Sp, compared to that of the control group (**Figure 2B**). Notably, treatment with curcuin for GIOP mice resulted in increasing the BV/TV, Tb. N, Tb. Th and Tb. Sp (**Figure 2B**). To clarify the role of curcumin in bone metabolism further, TRAP staining was performed to clarify the activity of osteoclasts in the proximal metaphysis of tibia. The results indicated that TRAP-positive stained area (red) was a significantly increased in the tibia of GIOP rat as compared to that of the control group. The curcumin supplement significantly decreased the TRAP-positive stained area in the GIOP mice (**Figure 3A** and **3B**). OPG/RANKL/RANK cytokine system is essential for osteoclast biology. Various studies suggest that metabolic bone diseases are related to alterations of this system. Therefore, the mRNA levels in the proximal metaphysis of tibia were measured. The mRNA levels of OPG were not changed, but RANKL and RANK levels were increased in GIOP mice as compared to that of the control group (**Figure 3C-E**). Intriguingly, curcumin could inhibit the activity of OPG/RANKL/RANK signaling in GIOP mice.

Involvement of miR-365 in DXM-induced RANKL, CTSK, MMP-13 and MMP-9 expression

We next studied the molecular mechanism by which miR-365 regulates osteoblast and osteoclast functions. Target prediction tools TargetScan, PicTar and microRNA.org were utilized in order to find out possible target genes for miR-365. We found that miR-365 regulated MMP-9 through the predicted binding sites in its 3'-UTR (**Figure 4A**). To test whether miR-365 can

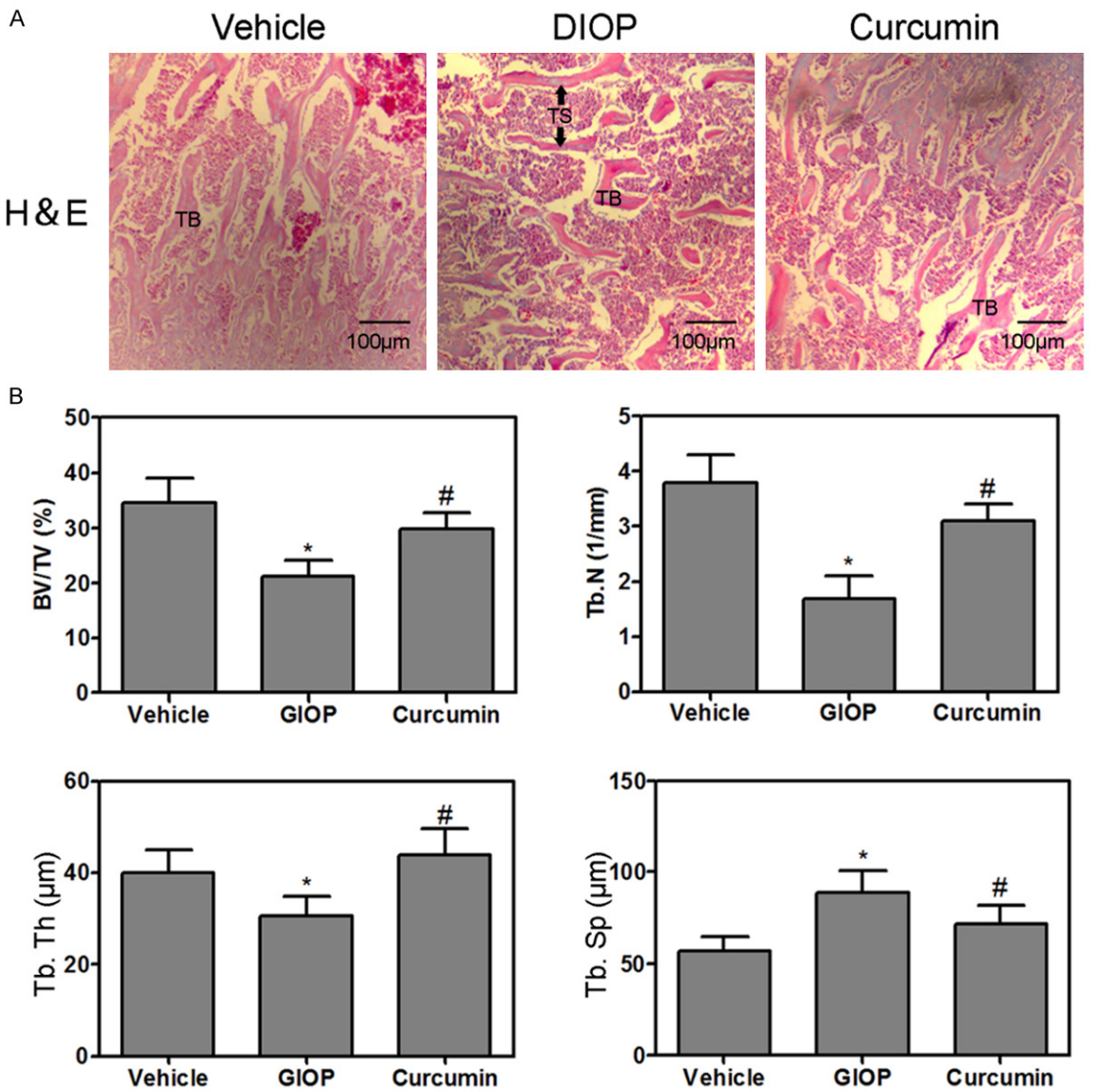

Figure 2. Hematoxylin and eosin staining of the proximal metaphysis of the tibia, trabecular bone zone below growth plate was shown (A: 50×). Bone volume over total volume (BV/TV), trabecula number (Tb. N), trabecula thickness (Tb. Th) and trabecula separation (Tb. Sp) were measured (B). Values were expressed as mean ± SD, n = 6 in each group. $^{*}P < 0.05$ versus vehicle group, $^{\#}P < 0.05$ versus GIOP group.

directly regulate MMP-9, a luciferase reporter construct containing the 3'-UTR of MMP-9 was used. In addition, a luciferase reporter construct containing mutations in the 3'-UTR of MMP-9 was also synthesized. The wild-type and mutant MMP-9 luciferase expression vectors were transfected with mimic miR-365 in calvarial osteoblast cells and the level of luciferase enzyme activity was measured. Overexpression of miR-365 suppressed the luciferase activity of the reporter gene. Mutation of three nucleotides within the miRNA binding site abolished this repression of luciferase activity confirming the specificity of the action (**Figure 4B**). Next, the regulation of miR-365 expression by DXM in osteoblasts, MC3T3-E1, osteoclasts and RAW 264.7 was measured. We observed that DXM caused a significant decrease of miR-365 expression in osteoblasts, MC3T3-E1, osteoclasts and RAW 264.7 (**Figure 4C** and **4D**). In addition, DXM also stimulated the expression of RANKL in osteoblasts and MC3T3-E1, however, miR-365 gain-of-function could inhibit the up-regulation of RANKL induced by

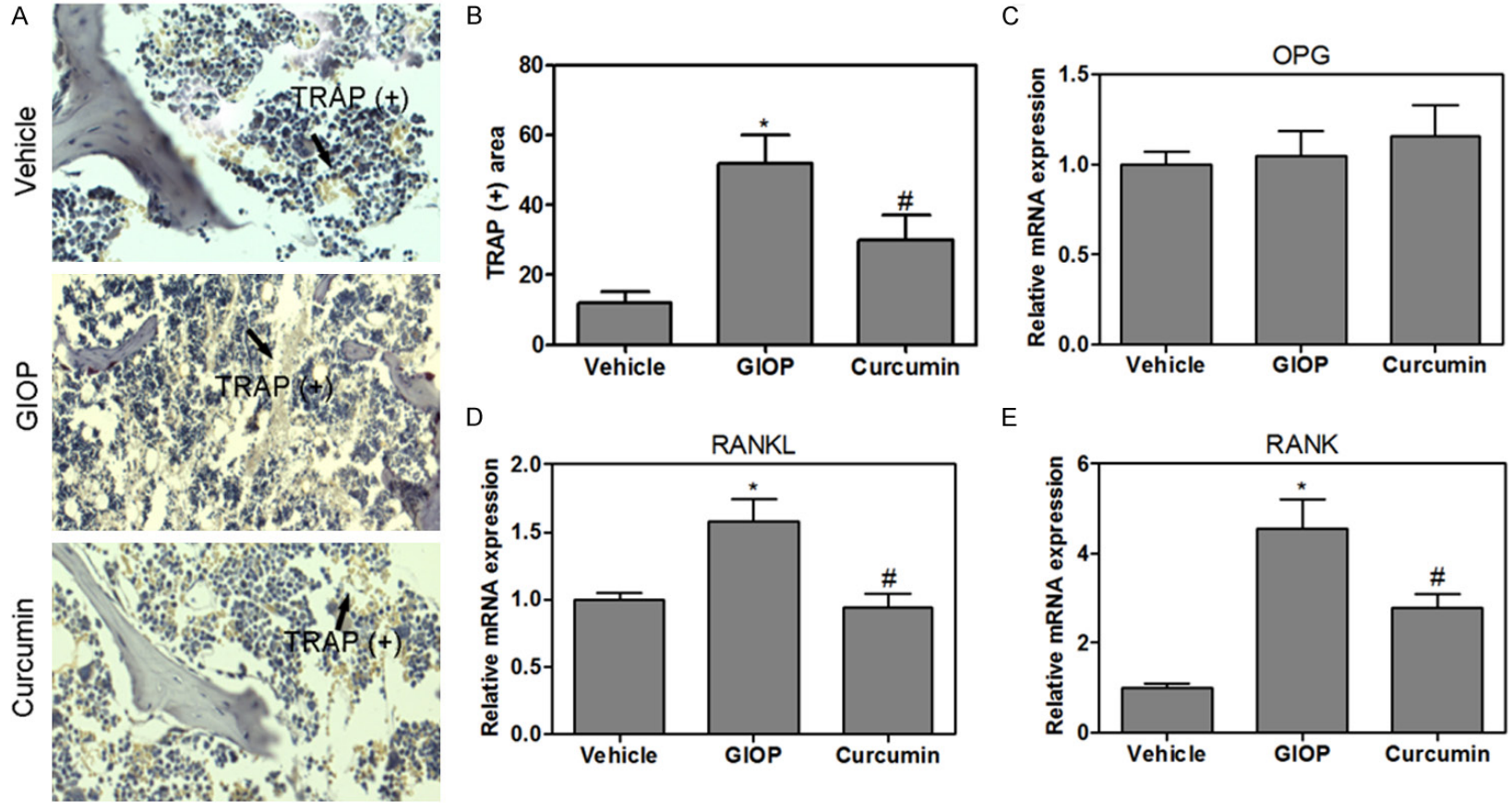

Figure 3. TRAP staining of the proximal metaphysis of the tibia (A) and the quantitative analysis of TRAP-positive stained area (B). Real-time PCR quantification of OPG (C), RANKL (D) and RANK (E) in the tibia of mice. Values were expressed as mean ± SD, n = 6 in each group. $^{*}P < 0.05$ versus vehicle group, $^{\#}P < 0.05$ versus GIOP group.

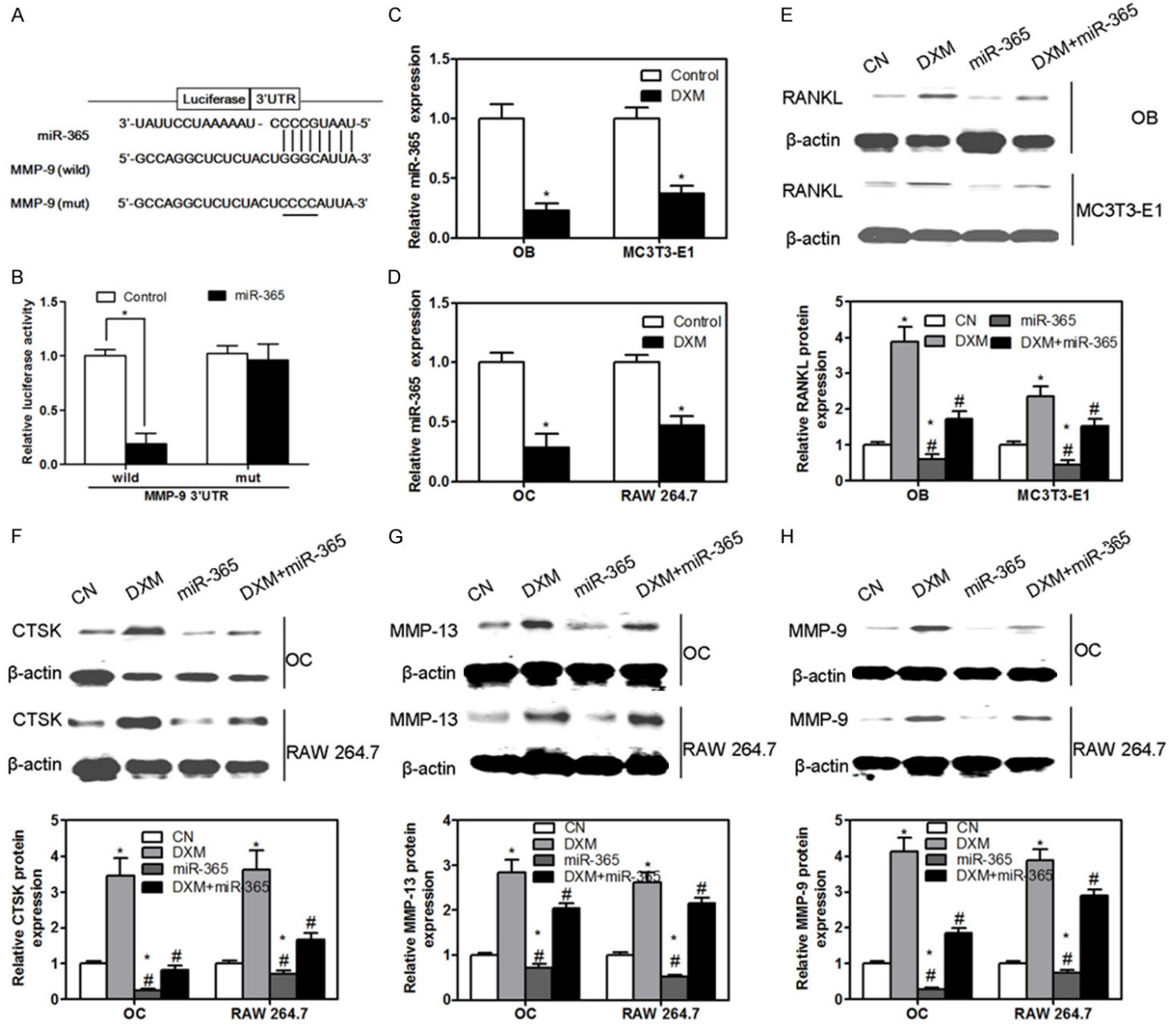
A
Luciferase
3'UTR
miR-365
3'-UAUUCCUAAAAAU-
CCCCGUAAU-5'
5'-GCCAGGCUCUCUACUGGGCAUUA-3'
MMP-9 (wild)
MMP-9 (mut)
5'-GCCAGGCUCUCUACUCCCCAUUA-3'
B
Control
miR-365
Relative luciferase activity
wild
mut
MMP-9 3'UTR
C
Control
DXM
Relative miR-365 expression
OB
MC3T3-E1
D
Control
DXM
Relative miR-365 expression
OC
RAW 264.7
E
CN
DXM
miR-365
DXM+miR-365
RANKL
β-actin
OB
MC3T3-E1
Relative RANKL protein expression
F
CTSK
β-actin
OC
RAW 264.7
Relative CTSK protein expression
G
MMP-13
β-actin
OC
RAW 264.7
Relative MMP-13 protein expression
H
MMP-9
β-actin
OC
RAW 264.7
Relative MMP-9 protein expression

Figure 4. Schematic representation of the putative miR-365 binding site in the MMP-9 3'UTR (A). Luciferase activity assay (B). The levels of miR-365 were measured in osteoblast (OB) and MC3T3-E1 in the present of DXM (C). The levels of miR-365 were measured in osteoclast (OC) and RAW 264.7 in the present of DXM (D). The protein expression of RANKL was measured by western blotting in osteoblast (OB) and MC3T3-E1 (E). The protein expression of CTSK (F), MMP-13 (G) and MMP-9 (H) was measured by western blotting in osteoclast (OC) and RAW 264.7. Values were expressed as mean ± SD, n = 3 in each group. $^{*}P < 0.05$ versus CN group, $^{\#}P < 0.05$ versus DXM group.

DXM administration (**Figure 4E**). Furthermore, DXM could increase the protein expression of CTSK, MMP-13 and MMP-9 in osteoclasts and RAW 264.7, however, co-application of miR-365 gain-of-function and DXM almost completely abolished the effect of DXM in the expression of CTSK, MMP-13 and MMP-9 (**Figure 4F-H**). Application of miR-365 gain-of-function alone decreased the levels of RANKL (**Figure 4E**) in osteoblasts and MC3T3-E1 and CTSK (**Figure 4F**), MMP-13 (**Figure 4G**) and MMP-9 (**Figure 4H**) in osteoclasts and RAW 264.7 as compare to control group. These results suggested that miR-365 gain-of-function could inhibit DXM-induced osteoclastogenesis through the suppression of RANKL expression in osteoblasts and directly regulate the bone resorption of osteoclasts.

MiR-365 is a regulator of curcumin for bone formation in vivo

In vivo studies, we found that the levels of miR-365 were suppressed in the tibia from GIOP mice (**Figure 5A**). In contrast, the mRNA and protein expression of CTSK, MMP-13 and MMP-9 were significantly higher in the tibia from GIOP mice than that of the control group (**Figure 5B-D**). The higher levels of CTSK and MMP-13 returned to the control value in the curcumin-supplemented GIOP mice. Interestingly, the levels of miR-365 was increased (**Figure 5A**), simultaneously, the mRNA and protein expression of MMP-9 were inhibited in the curcumin-supplemented GIOP mice (**Figure 5C** and **5D**).

Discussion

Bone homeostasis is maintained by osteoclast-mediated bone resorption and osteoblast-mediated bone formation. However, GCs can cause disequilibrium of bone homeostasis through the inhibition of osteoblastogenesis and the apoptosis of osteoblasts and osteocytes, which are considered to be the primary cause for bone deteriorations inducing by GCs [20]. Previous studies have revealed that GCs up-regulate the expression of RANKL and M-CSF in osteoblasts indirectly acting on the osteoclastogenesis. However, the molecular mechanisms of GCs-induced osteoblasts and osteoclasts dysfunction remain elusive. In the present study, we demonstrated that GCs could increase MMP-9 expression in osteoclasts directly enhancing osteoclastogenesis and bone resorption in GIOP mice. Intriguingly, curcumin as a new and effective drug had an inhibitory effect on bone resorption in GIOP mice. The effect of this compound was not only its ability to inhibit the activity of osteoclasts, but also its ability to stimulate the activity of osteoblasts and accelerate bone formation. In addition, the underlying mechanism of inhibiting bone resorption and accelerating bone formation by curcumin was mediated, at least partially, through the activation of microRNA-365 via suppressing MMP9.

MMP-9 is a zinc-dependent endopeptidase that participates in a variety of physiological and biochemical processes. In bone biology, MMP-9 is produced by osteoclasts and plays an important role in the degradation of extracellular matrix [21]. MMP-9 knockout mice exhibit altered growth plate vascularization and ossification during development and delayed repair of experimental induced bone fractures [22, 23]. Extracellular matrix (ECM) degradation by osteoclasts is a critical process in both normal bone remodeling and bone resorption inducing by bone diseases. Because it is highly expressed in osteoclasts, MMP-9 (type IV collagenase or gelatinase B) is a feasible candidate drug target of curcumin for regulating bone metabolism in experimentally GIOP mice. In our work, the mRNA and protein expression of MMP-9 were significantly higher in the tibia from GIOP mice than that of the control group. The higher levels of MMP-9 returned to the control value in the curcumin-supplemented GIOP mice. Therefore, we have reason to believe that curcumin could significantly ameliorate bone deteriorations in GIOP mice through the suppression of MMP-9. Moreover, cathepsin K as an activator of MMP-9 was investigated in GIOP mice. Cathepsin K is also highly expressed in

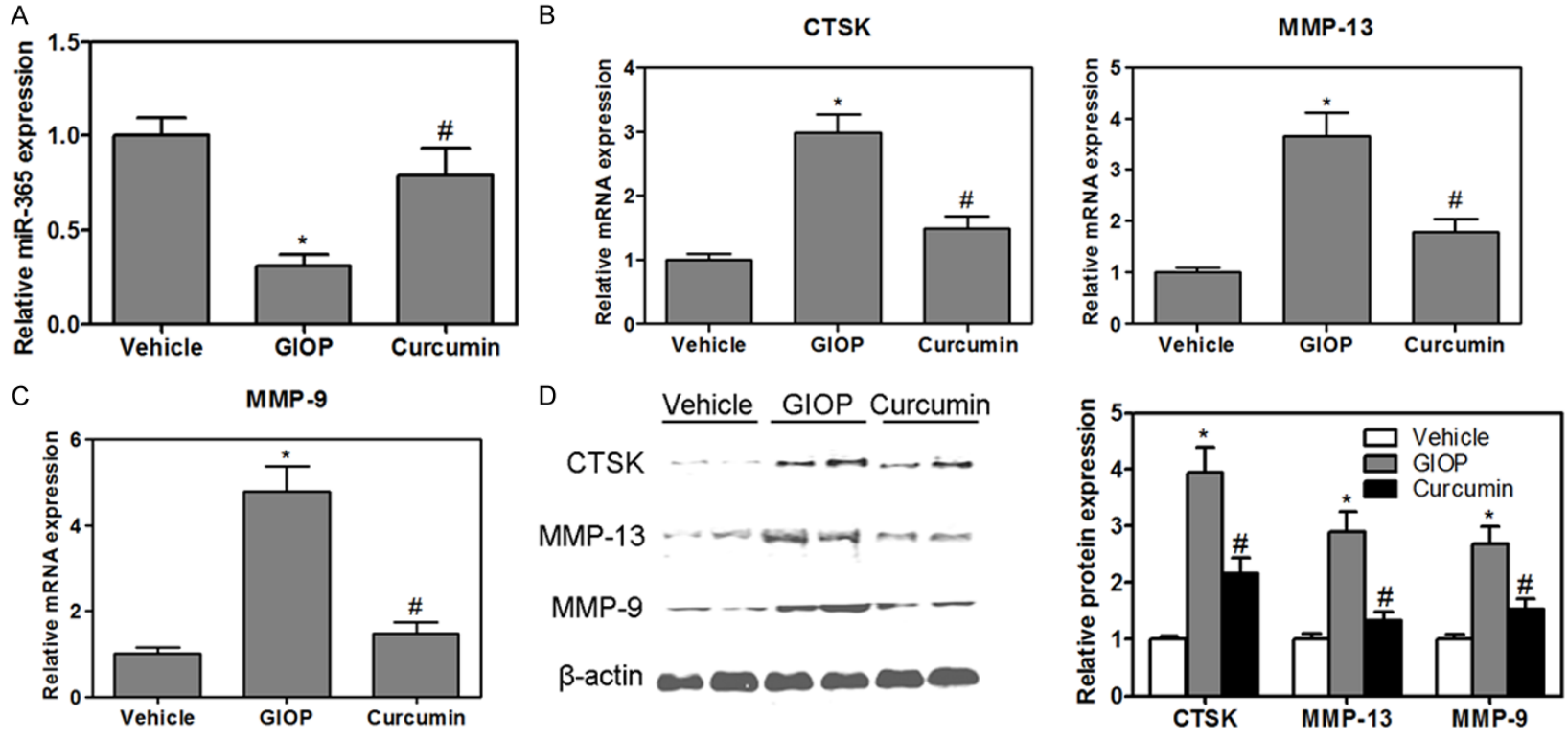

Figure 5. The levels of miR-365 were measured in the tibia of mice (A). The mRNA expression of CTSK and MMP-13 was measured in the tibia of mice (B). Gene expression of MMP-9 was measured by real-time PCR in the tibia of mice (C). Western blotting analysis of CTSK, MMP-13 and MMP-9 in the tibia of mice (D). Values were expressed as mean ± SD, n = 6 in each group. $^{*}P < 0.05$ versus vehicle group, $^{\#}P < 0.05$ versus GIOP group.

osteoclasts and synovial fibroblasts where it contributes to degradation of the ECM [24, 25]. Osteoclast-specific cathepsin K deletion stimulates S1P-dependent bone formation, in contrast, targeted deletion of cathepsin K in osteoblasts had no effect on bone resorption or bone formation rate [26]. Our data provided pharmacological evidence that the mRNA and protein expression of cathepsin K were increased in GIOP mice as compared to that of the control group. Curcumin could inhibit the upregulation of cathepsin K in GIOP mice.

Several miRs have been found to be related to GC-induced bone deteriorations. More recently, miR-29a protected against GC-induced disturbance of Wnt and Dkk-1 actions and improved osteoblasts differentiation and mineral acquisition [27]. Moreover, DXM acts on osteoblasts to up-regulate the expression of RANKL by decreasing microRNA-17/20a, which indirectly affects osteoclast differentiation and bone resorption [20]. In our study, microRNA as a target of drug action was investigated. MiR-365 as an upstream regulator of MMP-9 was selected to elaborate the pharmacological mechanisms for curcumin in experimentally GIOP mice. In vivo studies, we found that the levels of miR-365 were suppressed in the tibia from GIOP mice. Interestingly, the levels of miR-365 was increased, simultaneously, the mRNA and protein expression of MMP-9 were inhibited in the curcumin-supplemented GIOP mice. Therefore, we have reason to believe that curcumin could significantly ameliorate bone deteriorations in GIOP mice, and the underlying mechanism was mediated, at least partially, through the activation of miR-365 via suppressing MMP-9.

Disclosure of conflict of interest

None.

Address correspondence to: Dr. Rongkai Zhang, Department of Orthopaedics II, Fifth Affiliated Hospital of Sun Yat-sen University, 52 East Meihua Road, Zhuhai 519000, China. Tel: (86) 756-2528722; Fax: (86) 756-2528722; E-mail: rkzhang_fh@163.com

References

[1] Yao W, Dai W, Jiang L, Lay EY, Zhong Z, Ritchie RO, Li X, Ke H and Lane NE. Sclerostin-antibody treatment of glucocorticoid-induced osteoporosis maintained bone mass and strength. Osteoporos Int 2015; [Epub ahead of print].

[2] Weinstein RS. Glucocorticoid-induced osteoporosis. Rev Endocr Metab Disord 2001; 2: 65-73.

[3] Sato AY, Tu X, McAndrews KA, Plotkin LI and Bellido T. Prevention of glucocorticoid induced-apoptosis of osteoblasts and osteocytes by protecting against endoplasmic reticulum (ER) stress in vitro and in vivo in female mice. Bone 2015; 73: 60-68.

[4] Sun LN, Yang ZY, Lv SS, Liu XC, Guan GJ and Liu G. Curcumin prevents diabetic nephropathy against inflammatory response via reversing caveolin-1 Tyr14 phosphorylation influenced TLR4 activation. Int Immunopharmacol 2014; 23: 236-246.

[5] Kuncha M, Naidu VG, Sahu BD, Gadepalli SG and Sistla R. Curcumin potentiates the anti-arthritic effect of prednisolone in Freund's complete adjuvant-induced arthritic rats. J Pharm Pharmacol 2014; 66: 133-144.

[6] Moon HJ, Ko WK, Han SW, Kim DS, Hwang YS, Park HK and Kwon IK. Antioxidants, like coenzyme Q10, selenite, and curcumin, inhibited osteoclast differentiation by suppressing reactive oxygen species generation. Biochem Biophys Res Commun 2012; 418: 247-253.

[7] Hie M, Yamazaki M and Tsukamoto I. Curcumin suppresses increased bone resorption by inhibiting osteoclastogenesis in rats with streptozotocin-induced diabetes. Eur J Pharmacol 2009; 621: 1-9.

[8] Oh S, Kyung TW and Choi HS. Curcumin inhibits osteoclastogenesis by decreasing receptor activator of nuclear factor-kappaB ligand (RANKL) in bone marrow stromal cells. Mol Cells 2008; 26: 486-489.

[9] Hussan F, Ibraheem NG, Kamarudin TA, Shuid AN, Soelaiman IN and Othman F. Curcumin Protects against Ovariectomy-Induced Bone Changes in Rat Model. Evid Based Complement Alternat Med 2012; 2012: 174916.

[10] French DL, Muir JM and Webber CE. The ovariectomized, mature rat model of postmenopausal osteoporosis: an assessment of the bone sparing effects of curcumin. Phytomedicine 2008; 15: 1069-1078.

[11] Kim WK, Ke K, Sul OJ, Kim HJ, Kim SH, Lee MH, Kim HJ, Kim SY, Chung HT and Choi HS. Curcumin protects against ovariectomy-induced bone loss and decreases osteoclastogenesis. J Cell Biochem 2011; 112: 3159-3166.

[12] Yang MW, Wang TH, Yan PP, Chu LW, Yu J, Gao ZD, Li YZ and Guo BL. Curcumin improves bone microarchitecture and enhances mineral density in APP/PS1 transgenic mice. Phytomedicine 2011; 18: 205-213.

[13] Sun X and Zhang J. Identification of putative pathogenic SNPs implied in schizophrenia-as-

sociated miRNAs. BMC Bioinformatics 2014; 15: 194.
[14] De Felice B, Manfellotto F, Palumbo A, Troisi J, Zullo F, Di Carlo C, Di Spiezio Sardo A, De Stefano N, Ferbo U, Guida M and Guida M. Genome-wide microRNA expression profiling in placentas from pregnant women exposed to BPA. BMC Med Genomics 2015; 8: 56.
[15] Li Z, Hassan MQ, Jafferji M, Aqeilan RI, Garzon R, Croce CM, van Wijnen AJ, Stein JL, Stein GS and Lian JB. Biological functions of miR-29b contribute to positive regulation of osteoblast differentiation. J Biol Chem 2009; 284: 15676-15684.
[16] Li H, Xie H, Liu W, Hu R, Huang B, Tan YF, Xu K, Sheng ZF, Zhou HD, Wu XP and Luo XH. A novel microRNA targeting HDAC5 regulates osteoblast differentiation in mice and contributes to primary osteoporosis in humans. J Clin Invest 2009; 119: 3666-3677.
[17] Hu R, Liu W, Li H, Yang L, Chen C, Xia ZY, Guo LJ, Xie H, Zhou HD, Wu XP and Luo XH. A Runx2/miR-3960/miR-2861 regulatory feedback loop during mouse osteoblast differentiation. J Biol Chem 2011; 286: 12328-12339.
[18] Cheng P, Chen C, He HB, Hu R, Zhou HD, Xie H, Zhu W, Dai RC, Wu XP, Liao EY and Luo XH. miR-148a regulates osteoclastogenesis by targeting V-maf musculoaponeurotic fibrosarcoma oncogene homolog B. J Bone Miner Res 2013; 28: 1180-1190.
[19] Dou C, Zhang C, Kang F, Yang X, Jiang H, Bai Y, Xiang J, Xu J and Dong S. MiR-7b directly targets DC-STAMP causing suppression of NFATc1 and c-Fos signaling during osteoclast fusion and differentiation. Biochim Biophys Acta 2014; 1839: 1084-1096.
[20] Shi C, Qi J, Huang P, Jiang M, Zhou Q, Zhou H, Kang H, Qian N, Yang Q, Guo L and Deng L. MicroRNA-17/20a inhibits glucocorticoid-induced osteoclast differentiation and function through targeting RANKL expression in osteoblast cells. Bone 2014; 68: 67-75.
[21] He B, Hu M, Li SD, Yang XT, Lu YQ, Liu JX, Chen P and Shen ZQ. Effects of geraniin on osteoclastic bone resorption and matrix metalloproteinase-9 expression. Bioorg Med Chem Lett 2013; 23: 630-634.
[22] Colnot C, Thompson Z, Miclau T, Werb Z and Helms JA. Altered fracture repair in the absence of MMP9. Development 2003; 130: 4123-4133.
[23] Vu TH, Shipley JM, Bergers G, Berger JE, Helms JA, Hanahan D, Shapiro SD, Senior RM and Werb Z. MMP-9/gelatinase B is a key regulator of growth plate angiogenesis and apoptosis of hypertrophic chondrocytes. Cell 1998; 93: 411-422.
[24] Hou WS, Li Z, Gordon RE, Chan K, Klein MJ, Levy R, Keysser M, Keyszer G and Bromme D. Cathepsin k is a critical protease in synovial fibroblast-mediated collagen degradation. Am J Pathol 2001; 159: 2167-2177.
[25] Wilson SR, Peters C, Saftig P and Bromme D. Cathepsin K activity-dependent regulation of osteoclast actin ring formation and bone resorption. J Biol Chem 2009; 284: 2584-2592.
[26] Lotinun S, Kiviranta R, Matsubara T, Alzate JA, Neff L, Luth A, Koskivirta I, Kleuser B, Vacher J, Vuorio E, Horne WC and Baron R. Osteoclast-specific cathepsin K deletion stimulates S1P-dependent bone formation. J Clin Invest 2013; 123: 666-681.
[27] Wang FS, Chuang PC, Lin CL, Chen MW, Ke HJ, Chang YH, Chen YS, Wu SL and Ko JY. MicroRNA-29a protects against glucocorticoid-induced bone loss and fragility in rats by orchestrating bone acquisition and resorption. Arthritis Rheum 2013; 65: 1530-1540.